Journal of the Korean Nuclear Society
Volume 17, Number 1, March, 1985

Experimental Investigation of Parametric Effects on the Void Fraction Measurement and Flow Regime Characterization by Capacitance Transducers

——Part I: Stationary Test——

Moon-Hyun Chun and Chang-Kyung Sung

Korea Advanced Institute of Science and Technology

(Received October 23, 1984)

캐패시턴스 변환기를 이용한 기포율 측정과 유동영역결정에 미치는 각종변수의 영향에 관한 실험적연구

——제 1 부 : 적정실험결과——

전 문 헌·성 창 경

한국과학기술원

(1984. 10. 23 접수)

Abstract

The main purpose of this work is to study the effects of (1) configuration, size, and materials of electrodes, (2) flow pattern, (3) electrode position with respect to a dielectric boundary on the void fraction measurement and flow regime characterization by capacitance transducers. From the experimental results, relationships between the measured relative capacitance and void fraction are obtained for both annular and stratified flow systems under static condition, and this result is compared with theoretical predictions. From this study it can be concluded that (1) the strip-type electrodes are more sensitive than ring-type electrodes for both annular and stratified flows, (2) electrode size does not affect the relative capacitance vs. $(1-\alpha)$ curve, and (3) electrode position is important for stratified flows but it has no effect on annular flows.

요 약

본 연구의 주목적은 (1) 전극의 모양, 크기 및 재질, (2) 유동형태, 그리고 (3) 유전경계(dielectric boundray)에 대한 전극의 상대적 위치 등이 캐패시턴스변환기를 이용한 기포율 측정과 유동영역 결정에 어떠한 영향을 미치는가를 연구하는 데에 있다. 실험 결과로부터 정적인 상태하에서 annular flow와 층류계(stratified flow system)에 대하여, 측정한 상대 캐패시턴스(relative capacitance)와 기포율과의 상관 관계를 구하였다. 그리고, 이 결과를 이론적 예측치와 비교하였다. 이 연구 결과로부터 다음과 같은 결론을 얻었다. 즉 (1) annular flow와 stratified flow의 경우 모두 strip-type의 전극이 ring-type의 전극보다 더 민감하다. (2) 전극의 크기는 상대적 캐패시턴스 대$(1-\alpha)$곡선에 아무런 영향을 미치지 않는다. (3) 전극의 위치는 stratified flow에 대해서는 중요하나 annular flow에 대해서는 아무런 영향이 없다.

Nomenclature

C	total (or output) capacitance of a system
C^*	relative capacitance defined by Eqs. (1) and (2)
C_1	capacitance of the tube completely filled with liquid or solid (i.e., when $\alpha=1$)
C_0	capacitance of the empty tube (i.e., when $\alpha=O$)
D	inside diameter of the test section (or outside diameter of the flow model shown in Fig. 2)
H	height shown in Fig. 2(b)
l	length of electrodes (in axial direction)
t	gap (or space) between two electrodes
w	width of electrodes
α	void fraction
ε	permittivity
ε_R	dielectric constant (or relative permittivity)
θ	stratified angle shown in Fig. A-1

Subscripts

1	material 1
2	material 2

I. Introduction

The response of the volumetric concentration of the liquid and vapor phases due to perturbations in heat flux and inlet flow is of particular interest due to its influence on the neutron dynamics in nuclear reactors(1). The problem of predicting void volumes for the flow of steam-water mixtures in vertical channels is important for the designer of boiling water reactors, in particular.

Most of the void measuring techniques which are based on the nuclear reactions such as gamma attenuation, X-ray attenuation, beta attenuation, neutron diffusion or the (γ, n) reaction are not applicable inside the teactor cores where intensive fields of all these nuclear radiations predominate (2). The disadvantages of γ-densitometry are that it exhibits a strong flow-regime dependence and requires a relatively strong source and thus, a large amount of radiation shielding, to observe fast transient phenomena (3).

Among the non-nuclear methods of void measurement one of the most important is the capacitance method, which is based on the difference between liquid and vapor dielectric constant. This measuring method has been applied to determine the void fraction in bulk boiling (2) and the particle velocity in gas-powder streams (3). The capacitance method has the following advantages (1, 3) : (1) most economical, (2) simple installation, (3) the electrodes are external to the flow, (4) applicable to fast transient phenomena, and (5) the output is an analog voltage suitable for process control.

The entire project of this work consists of (1) stationary experiments and (2) dynamic experiments. In our previous paper (1), a set of analytical relative capacitance formulas for core and anular flows was presented along with the formulas derived for stratified flows (one for horizontal electrode position and the other for vertical electrode position). In addition, only a part of the stationary test results was presented to examine the validity of the analytical formulas derived in the present work.

The main purpose of this paper, on the other hand, is to present the outline of the experimental techniques used and the experimental results to examine the effects of (1) geometry, size, and materials of electrodes, (2) flow patterns, and (3) electrode position with respect to a dielectric boundary on the measurement of void fraction by the capacitance technique.

II. Principles of Void Fraction Measurement by a Capacitance Transducers

The void fraction measurement technique is based upon the fact that the dielectric constant of the liquid water is a well defined parameter which is predominantly a function only of temperature and the value of the dielectric constant of the liquid (or solid phase) is very large compared to that of the gaseous phase. Depending on the flow pattern and size of bubbles, the total dielectric constant of a two-phase mixture (in the forced convection boiling) can be calculated as a function of the dielectric constants of the two media by means of theoretical relation (1, 2). One of these is the slug-flow law according to which the two slugs of vapor and liquid from an electrical viewpoint are in parallel between the electrodes. Another possible method of relating α to the relative capacitance C/C_0 is the Maxwell law (2). Also, in the case of annular flow regime it is possible to derive a function $\alpha=\alpha(C/C_0)$, by considering the liquid and vapor phases as capacitances in series. When the flow pattern corresponds to spray-flow regime, i.e., small liquid masses dispersed in a vapor matrix, another function $\alpha=\alpha\ (C/C_0)$ can be obtained by deriving the dielectric constant of the mixture by means of the Maxwell formula, applied for water droplets dispersed in a steam matrix.

III. Experimental Techniques

1. Experimental Apparatus

Two series of experiments were designed: one stationary experiments(i.e., experiments conducted under no flowing condition, at room temperature and at atmospheric pressure), the other dynamic experiments. As a first part of the series, stationary experiments were first carried out. The apparatus of the present stationary experiment consists of three major parts as shown in Fig. 1, 2, and 3.: (1) two types of test sections, one with a pair of strip-type electrodes (Fig. 3a), the other with a pair of ring-type electrodes (Fig. 3b), (2) simulation models for various void fraction and flow patterns (Fig. 2a, b), and (3) measuring equipment for capacitance.

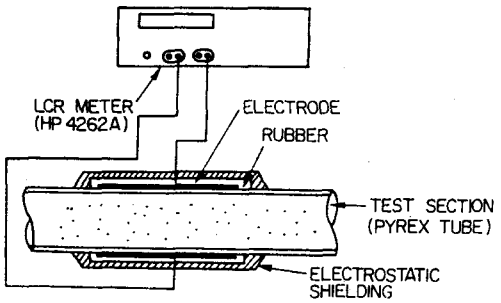

Fig. 1. Schematic Diagram of Experimental Apparatus

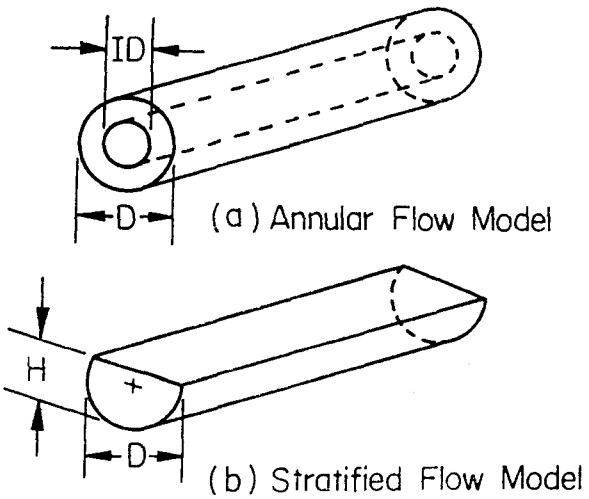

Fig. 2. Isometric Views of Flow Pattern Model

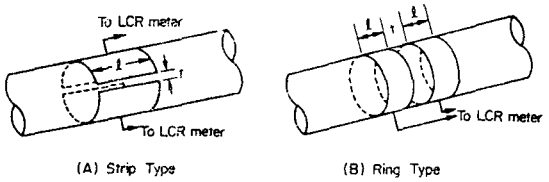

Fig. 3. Isometric Views of Two Different Electrode Configurations

Table 1. Test Section Geometry and Other Data

(a) Test Section Dimensions:

Material	I.D.(mm)	O.D.(mm)	Length(mm)	Volume(cc)	Test section No.
Pyrex Tube	34.5	38.5	250	234	Tube-1
Pyrex Tube	26	30	250	133	Tube-2

(b) Electrode Dimensions Attached to Each Test Section

Electrode Type	Material and Electrode No.	Width W(mm)	Length l(mm)	Gap t(mm)	Attached Test Section	Flow Model Material
Strip	Al-1	46	40	4	Tube-2	polyacrylate; water
	Al-2	46	50	4	Tube-2	polyacrylate
	Al-3	46	57	5.6	Tube-2	paraffin wax
	Al-4	46	60	3.5	Tube-2	polyacrylate
	Al-5	60	70	4	Tube-1	water
	Al-6	46	80	3.75	Tube-2	water
	Al-7	46	99	5.5	Tube-2	paraffin wax
	Cu-1	46	50	3.5	Tube-2	water; polyacrylate
	Cu-2	46	60	4	Tube-2	water
	Cu-3	60	45	3.5	Tube-1	water
Ring	Al-R	94	10		Tube-2	polyacrylate

The test section is a cylindrical pyrex tube where a pair of electrodes is attached circumferentially and then a simulation model is inserted. This was wrapped with a rubber sheet (lmm thick) and then electrostatically shielded with an aluminium foil as shown in Fig. 1. Dimensions of test sections and electrodes are given in Table 1.

Two basic electrode configurations designated as "ring" and "strip" were examined in the present test for sensitivity and flow regime dependency. Two isometric views of a pair of strip-type and a pair of ring-type electrodes wrapped around a pyrex tube are shown in Figs. 3(a) and 3(b). Test section dimensions are summarized in Table 1(a).

Dimensions of electrodes attached to each test section, on the other hand, are summarized in Table 1(b): e.g., the strip electrodes designated as "Cu-2" is made of a thin copper plate and consisted of two 60mm long by 46mm wide strips attached longitudinally and separated by 4mm (shown in Fig. 3a). The ring electrodes, on the other hand, consisted of two 10mm wide aluminium strips attached circumferentially to the tube(30mm outside diameter) and separated by 10mm (shown in Fig. 3b).

The void fraction and flow pattern, such as annular or stratified flow in the static condition, were controlled and simulated by inserting a known amount of water or by inserting a different simulation model (shown in Figs. 2a and 2b) with a known size into the test section. In the case of stratified flow, in particular, the void fraction was controlled by inserting known amount of water and also by changing the cross sectional height (H in Fig. 2b) of semi-circular cylinder. Dimensions and dielectric constants of flow pattern models are shown in Tables 2(a) and 2(b).

The output capacitance was measured with a digital LCR meter (HP model 4262A) that has the measuring range of capacitance from 0.01 pF to 19.99 mF. The LCR meter has a basic accuracy of 0.2 to 0.3% depending on test signal level, frequency and measuring equivalent

Table 2. Dimensions and Dielectric Constants of Flow pattern Models

(a) Dimensions of Flow Pattern Models

Flow Pattern	Model No.	D (Fig. 6) (mm)	ID (or H) (Fig. 2) (mm)	Void Fraction	Flow Model Material
Annular	A-1	26	0	0	paraffin wax
	A-2	〃	4.5	0.03	〃
	A-3	〃	8.04	0.14	〃
	A-4	〃	15.85	0.42	〃
	A-5	〃	18.9	0.51	〃
Annular	B-1	〃	0	0	polyacrylate
	B-2	〃	8.46	0.11	〃
	B-3	〃	11.68	0.20	〃
	B-4	〃	13.12	0.25	〃
	B-5	〃	16.20	0.39	〃
	B-6	〃	20.42	0.61	〃
	B-7	〃	23.02	0.79	〃
Stratified	C-1	〃	26	0	〃
	C-2	〃	20.17	0.17	〃
	C-3	〃	18.11	0.26	〃
	C-4	〃	15.10	0.40	〃
	C-5	〃	13.45	0.48	〃
	C-6	〃	12.11	0.54	〃

(b) Dielectric Constants of Flow Pattern Material[4]

Material	Dielectric Constant ε_R	Temperature (°C)
water	78.2	25
	55	102
Air	1	102
Paraffin wax	2.25	25
Polyacrylate	2.75	23

circuit.

2. Test Parameters and Test Procedures

The main controllable test parameters were: (1) flow pattern (annular and stratified), (2) electrode type (strip or ring) and its position on the test section with respect to the dielectric boundary (vertical or horizontal), (3) void fraction (from zero to unity), (4) test section diameter. These test parameters can be further classified as shown in Table. 3. It should be noted here that the definitions of the "horizontal electrode position" and the "vertical electrode position" are given in Appendix.

As may be observed in the relative capacitance formulas derived in our earrlier work (**1**), the relative capacitance is functions of dielectric constants ε_R, and void fraction α, except for the case of stratified flows with a pair of vertical strip-type electrods. Void fractions and flow patterns were simulated with a proper combination of two different materials having different dielectric constants.

In the preliminary test, the sensitivity and flow regime dependency of two basic electrode types (i.e., ring and strip type) were first examined and evaluated along with the sensitivity of LCR meter frequency. As a result, LCR meter frequency of 10 KHz and the strip-type electrode were selected to be used in all the final series of tests.

For each test, the following procedure is required:

1. The lead cable from a pair of electrodes is first connected to the LCR meter as shown in Fig. 1.

2. The capacitance of the leads and the empty tube (i.e., C_0) is then measured along with the capacitance of the leads and the tube which is completely filled with void fraction simulant material or flow pattern simulant material (i.e., C^1).

3. The output capacitance of the whole test section partially filled with a given void fraction or flow pattern model (i.e., C), which has a known dielectric constant and volume, is measured.

4. An experimental value of the relative capacitance C* is then obtained by substituting the above measured values of C, C_0, and C_1 into one of the following equations (**1**):

$$C^*=\frac{C-C_0}{C_1-C_0} \quad (\text{when } \varepsilon_1>\varepsilon_2) \tag{1}$$

$$C^*=\frac{C-C_1}{C_0-C_1} \quad (\text{when } \varepsilon_1<\varepsilon_2) \tag{2}$$

Table 3. Classification of Main Test Parameters

Test Parameters	Flow Pattern	Electrode	Void Fraction	Test Section Size
(1) Types	a) Annular flow b) Stratified flow	a) Ringtype b) Striptype	N/A	a) Tube-1 b) Tube-2
(2) Material or combination of simulation material:	a) Paraffin wax and air b) Polyacrylate and air c) Water and air	a) Aluminium b) Copper	N/A	Pyrex Tube
(3) Size or Range of measurement:	N/A	Listed in Table 1(b)	$\alpha=0\sim1$	Listed in Table 1(a)
(4) Position of electrode with respect to dielectric boundary	N/A	a) Horizontal b) Vertical c) 80 degree	N/A	N/A

where

$$C_0=[C]_{\alpha=0}=\frac{\pi\varepsilon 2l}{2} \tag{3}$$

$$C_1=[C]_{\alpha=1}=\frac{\pi\varepsilon 1l}{2} \tag{4}$$

It may be noted here that the "relative capacitance" is defined as in Eqs. (1) and (2) to eliminate capacitances of the connecting cables and the pyrex tube.

IV. Experimental Results and Discussion

From the experimental results, relationships between the measured relative capacitance (C^*) of the strip and ring electrodes and void fraction (in the form of $1-\alpha$) in annular and stratified flow systems under static condition are obtained for various combinations of thst parameters, and this result is compared with theoretical predictions. A brief summary of important results is as follows:

1. Flow Regime Dependence of c vs. $(1-\alpha)$ Curve. Sensitivities of Ring and Strip Electrodes, and the Necessity of Flow Regime Characterization

The flow regime dependence of the "output capacitance (C-C_0) vs. ($1-\alpha$) curve" is shown in Fig. 4 for both ring and strip electrodes. From this figure one may observe that the strip electrodes are, in general, far more sensitive than ring electrodes for both annular and stratified flows. Therefore, the strip-type elec-

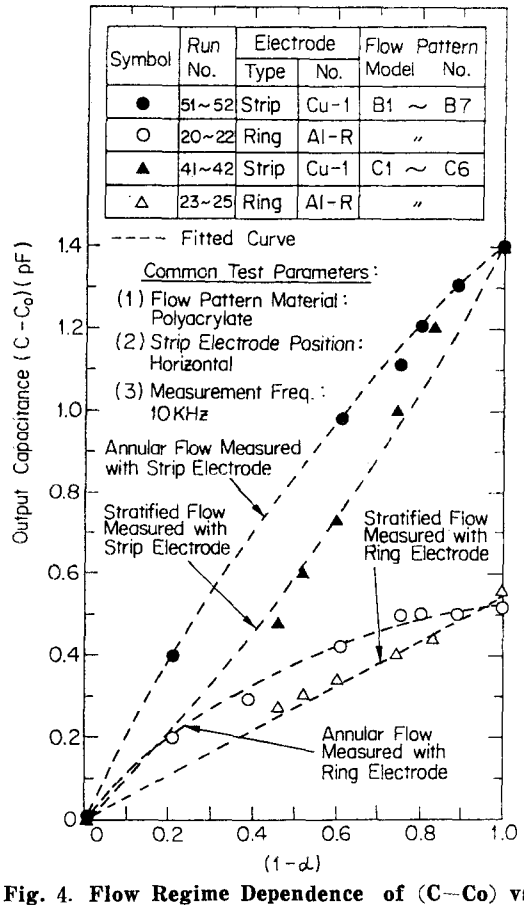

Fig. 4. Flow Regime Dependence of (C—Co) vs. $(1-\alpha)$ Curve and Sensitivities of Ring and Strip Electodes

trodes are employed in all the test of other parameters in this work.

It should be noted here that the void fraction cannot be determined without independent knowledge of the flow pattern. Therefore, it is necessary to determine the flow pattern of the given two-phase system before making the void fraction measurement by means of the capacitance transducer technique. For the flow regime characterization, on the other hand, one may be able to construct as many calibration curves as necessary in a manner similar to the methods used to obtain the curves shown in Fig. 4; in Fig. 4, one can observe that the two flow patterns (i.e., an annular flow and a stratified flow) are characterized by the two entirely different $(C\text{-}C_0)$ versus$(1\text{-}\alpha)$ curves depending only on the electrode types.

2. Effect of the Electrode Size and Flow Pattern Materal on C^* vs. $(1-\alpha)$ Curve

Fig. 5 shows that C^* vs. $(1\text{-}\alpha)$ curve depends on the flow pattern material, but does not depend on the electrode size, whereas the output capacitance $(C\text{-}C_0)$ increases with increase in electrode size. The sensitivity of C can be improved by using larger electrodes.

3. Effect of Electrode Configuratio on C^* vs. $(1-\alpha)$ Curve

Reproducibility and the effect of strip-type electrodes position on the C^* vs. $(1\text{-}\alpha)$ curve for annular and stratified flows are shown in Figs. 6 and 7, respectively. While Fig. 6 indicates that the C^* vs. $(1\text{-}\alpha)$ curve does not depend on electrodes position for annular flow, Fig. 7 shows that it depends on the electrode position for stratified flow. Also, Fig. 7 shows that the vertical electrode position gives larger values of C^* than the horizontal electrode position for stratified flows.

As can be noticed in Fig. 6, there is some deviation between the measured values of the relative capacitance C^* for a given condition. The maximum deviation between the values of the different measurement is about 20% of

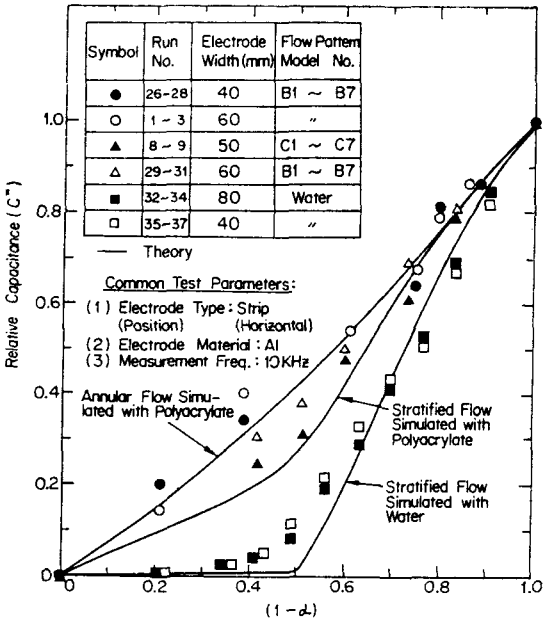

Fig. 5. Effect of Electrode Size and Flow Pattern Material on C^* vs. $(1-\alpha)$ Curve

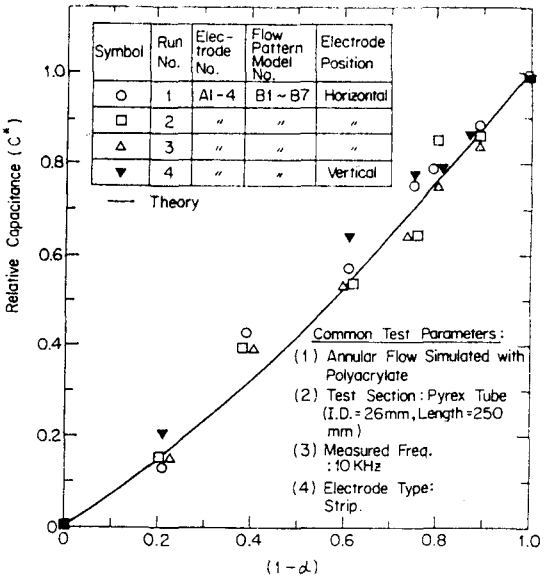

Fig. 6. Reproducibility and Effects of Electrode Position on C^* vs. $(1-\alpha)$ Curve for Annular Flow

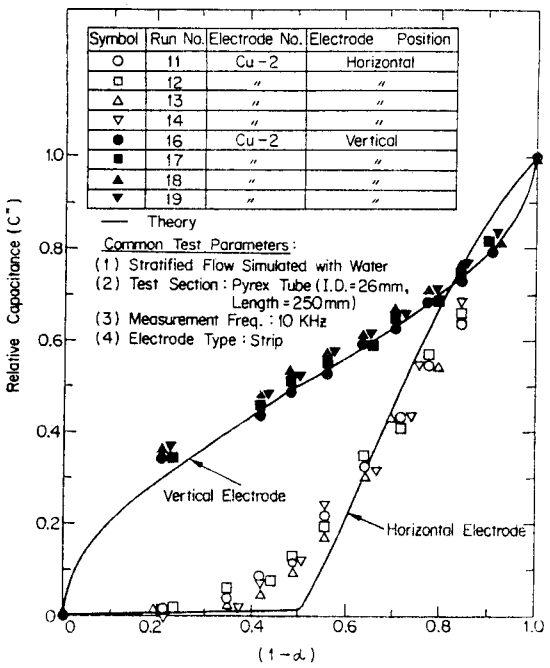

Fig. 7. Reproducibility and Effects of Electrode Position on C^* vs. $(1-\alpha)$Curve for Stratified Flow

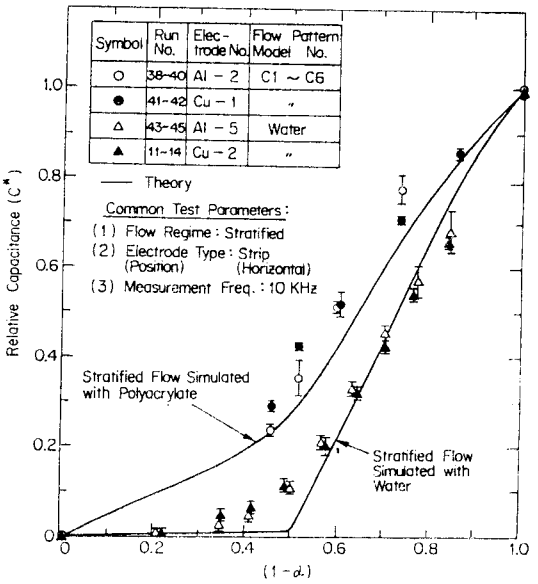

Fig. 8. Effects of Electrode Material on C^* vs. $(1-\alpha)$ Curve

the measured values.

4. Effect of Electrode Material on C^* vs. $(1-\alpha)$ Curve

Two materials for strip electrodes (i.e., Al and Cu) are tested to evaluate the sensitivity and possible effects of electrode material on the measurement of C^* vs. $(1-\alpha)$. However, no visible effect can be observed from the experimental results shown in Fig. 8.

5. Accuracy of the Results

To evaluate approximately the accuracy of the results obtained with the capacitance method, measured values of $(1-\alpha)$ are compared with true values of $(1-\alpha)$ as shown in Fig. 9. The predicted values $(1-\alpha)$ in Fig. 9 are obtained by substituting the relative capacitance measured by a capacitance transducer into the theoretical formulas derived in the previous work (such as Eqs. 9b, 10, or 11 in Ref. 1). True values of $(1-\alpha)$, on the other hand, correspond to those

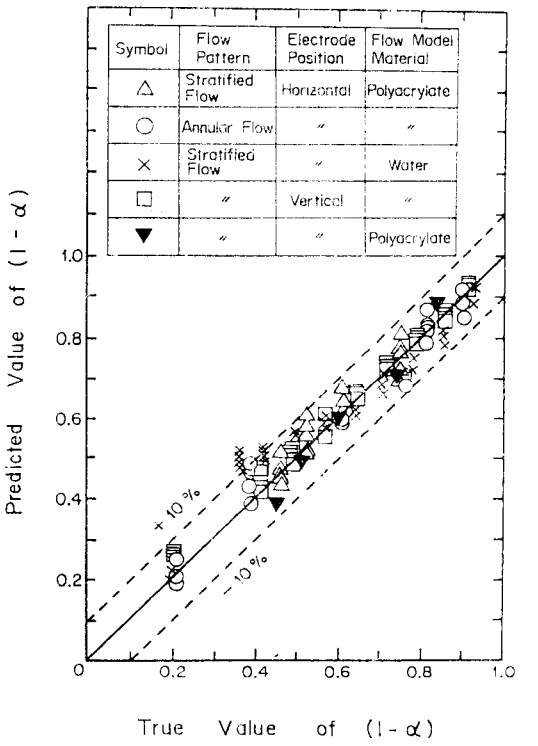

Fig. 9. Comparison of Experimental and True $(1-\alpha)$ Value

values simulated by inserting a different simulation model with known size (listed in Table 2) into the test section (or controlled by inserting known amount of water into the test section).

As can be seen in Fig. 9, the agreement between the predicted values and true values is within±10% with some exceptions of the results that were obtained for stratified flow simulated with water at lower $(1-\alpha)$ values than 0.5. In Fig. 5, it must be noticed that when stratified flow is simulated by water (and air), in particular, the slope of the C^* vs. $(1-\alpha)$ curve is extremely small until $(1-\alpha)$ value reaches 0.5; the main reason for this is because there is a large difference in dielectric constants of water (55 at 102°C) and air (1 at 102°C) as shown in Table 2(b). Also, in the theoretical formulas shown in the Appendix (Eqs. A-1 and A-2), it should be noticed that Eq. (A-1) is applicable for $0 \leqq \theta \leqq \frac{\pi}{2}$, whereas Eq. (A-2) is applicable for $\frac{\pi}{2} \leqq \theta \leqq \pi$. The region of small $(1-\alpha)$ values (i.e., from 0 to 0.5) corresponds to $0 \leqq \theta \leqq \frac{\pi}{2}$. Consequently, small fluctuations in measurements due to finite precision of instruments used in making the capacitance measurements can introduce large relative errors in the region of small $(1-\alpha)$ values.

Instrumental errors of the present work are mainly associated with the accuary of the LCR meter (HP model 4262 A); the accuracy of the LCR meter is 3% of the reading plus counts according to its specifications.

6. Problems to be Resolved for Practical Applications

Clearly, the above results and discussions apply to the stationary condition. However, in a flow situation, the interface between gas/vapor-liquid is not well defined. Therefore, a question will arise: how such a change will affect the comparison between observed and predicted values of the void fraction? In addition, pulsations, turbulence, wave motions, and non-uniform annular film thickness could be present in actual dynamic liquid-gas/vapor system. This paper is concerned with the stationary test results only. Those problems that are concerned with the dynamic conditions will be properly addressed in our next paper on the dynamic test which is now under preparation. Construction of a test loop for dynamic experiments has been already completed and also a series of dynamic experiments has been carried out at the KAIST.

V. Conclusions

From the present experimental results and comparisons with the theory (1) following conclusions can be made:

1. Strip-type electrodes are more sensitive than ring electrodes for both annular and stratified flows.

2. Electrodes size does not affect the relative capacitance vs. $(1-\alpha)$ curve, but the sensitivity of the output capacitance (C) can be improved by increasing the electrode size.

3. Electrode position is important for stratified flows, but is has no effect on annular flows. Since the vertical electrode position giveslarger values of C^* than the horizontal electrode position, the vertical electrode position should be used for stratified flows in particular.

4. In general, the agreement between the predicted values of $(1-\alpha)$ and the experimental results is within ±10 percent.

5. Without independent knowledge of the flow pattern the void fraction cannot be determined. Therefore, it is necessary to determine the flow pattern of the given two-phase flow system before making the void fraction measurement by means of the capacitance transducer

technique.

6. In a flow situation, the interface between gas/vapor-liquid is not well defined. In addition, pulsations, turbulence, wave motion and non-uniform annular film thickness could be present in actual dynamic liquid-gas system. To address these problems, a small loop for dynamic experiments has been constructed. A series of tests has been completed under the condition of a two-phase mixture in forced convection for different values of void fractions and flow rates. The manuscript of the paper on the dynamic experiments is now under preparation.

Acknowledgements:

This work was supported by the Korea Science and Engineering Foundation.

References

1. M.H. Chun and C.K. Sung, "Flow Regime Characterization and Void Fraction Measurement by Capacitance Transducers," ASME Paper 84-WA/HT-56 (1984).
2. L. Cimorelli, and R. Evangelisti, "The Application of the Capacitance Method for Void Fraction Measurement in Bulk Boiling Conditions," *Int. J. Heat Mass Transfer*, Vol. 10, pp. 277-288 (1978).
3. G.A. Irons, and J.S. Chang, "Measurement of Void Fraction and Particle Velocity in Gas-Powder Streams by Capacitance Transducers," *Int. J. Multiphase Flow* (1983).
4. A.R.V. Hippel, "Dielectric Materials and Applications," MIT Press, MIT.

Appendix

1. Definitions of the "Horizontal Elecrtode Position" and the "Vertical Electrode Position"

For stratified flows, there are two typical configurations depending on the position of strip-type electrodes with respect to the dielectric boundary as shown in Fig. A-1. The following two terms are defined for convenience in discussion:

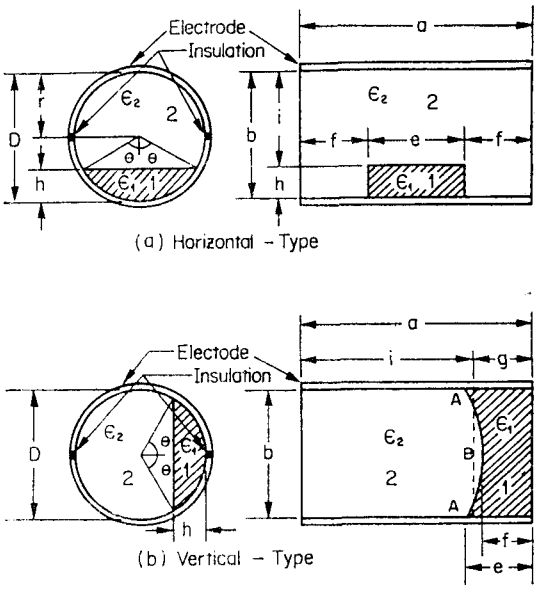

Fig. A-1. Cross Section of Two Test Sections with aPair of Strip-Type Electrodes for Stratified Flows

"Horizontal Electrode Position"—This is the case when the dielectric boundary (i.e., the interface between the two different materials with perimittivities of ε_1 and ε_2) is parallel to the imaginary line connecting two insulation points between a pair of strip electrodes attached circumferentially on the surface of a test section (Fig. A-1a).

"Vertical Electrode Position"—The configuration of strip electrodes is such that the dielectric boundary is vertical to the imaginary line joining two insulation points between a pair of electrodes (Fig. A-1b).

2. Relative Capacitance Formulas for Stratified Flows:

The theoretical formulas for the case of stra-

tified flows with a pair of horizontal strip-type electrodes were derived in our previous work (Ref. 1). For the horizontal position, in particular, the relative capacitance formulas for stratified flows are given by the following equations:

$$C^*=\frac{\varepsilon_{2R}\theta(1-\cos\theta)}{\varepsilon_{2R}\pi-(\varepsilon_{2R}-\varepsilon_{1R})\theta(1+\cos\theta)} \quad \left(\text{If } \varepsilon_{1R}>\varepsilon_{2R} \text{ and } 0\leq\theta\leq\frac{\pi}{2}\right) \tag{A-1}$$

$$C^*=\frac{\varepsilon_{1R}\pi+(\pi-\theta)[\varepsilon_{2R}(1-\cos\theta)-2\varepsilon_{1R}]}{\varepsilon_{1R}\pi+(\varepsilon_{2R}-\varepsilon_{1R})(\pi-\theta)(1-\cos\theta)} \quad \left(\text{If } \varepsilon_{1R}>\varepsilon_{2R} \text{ and } \frac{\pi}{2}\leq\theta\leq\pi\right) \tag{A-2}$$

In Eqs. (A-1) and (A-2), θ is the stratified angle shown in Fig. A-1.